PERK Activation at Low Glucose Concentration Is Mediated by SERCA Pump Inhibition and Confers Preemptive Cytoprotection to Pancreatic β-Cells

Claire E. Moore, Omotola Omikorede, Edith Gomez, Gary B. Willars, and Terence P. Herbert

Department of Cell Physiology and Pharmacology, The Henry Wellcome Building, University of Leicester, University Road, Leicester LE1 9HN, United Kingdom

Protein kinase R-like ER kinase (PERK) is activated at physiologically low glucose concentrations in pancreatic β-cells. However, the molecular mechanisms by which PERK is activated under these conditions and its role in β-cell function are poorly understood. In this report, we investigated, in dispersed rat islets of Langerhans and mouse insulinoma-6 (MIN6) cells, the relationship between extracellular glucose concentration, the free endoplasmic reticulum (ER) calcium concentration ($[Ca^{2+}]_{ER}$) measured directly using an ER targeted fluorescence resonance energy transfer-based calcium sensor, and the activation of PERK. We found that a decrease in glucose concentration leads to a concentration-dependent reduction in $[Ca^{2+}]_{ER}$ that parallels the activation of PERK and the phosphorylation of its substrate eukaryotic initiation factor-2α. We provide evidence that this decrease in $[Ca^{2+}]_{ER}$ is caused by a decrease in sarcoplasmic/ER Ca^{2+}-ATPase pump activity mediated by a reduction in the energy status of the cell. Importantly, we also report that PERK-dependent eukaryotic initiation factor-2α phosphorylation at low glucose concentration plays a significant role in 1) the regulation of both proinsulin and global protein synthesis, 2) cell viability, and 3) conferring preemptive cytoprotection against ER stress. Taken together, these results provide evidence that a decrease in the ATP/energy status of the cell in response to a decrease in glucose concentration results in sarcoplasmic/ER Ca^{2+}-ATPase pump inhibition, the efflux of Ca^{2+} from the ER, and the activation of PERK, which plays an important role in both pancreatic β-cell function and survival. **(*Molecular Endocrinology* 25: 315–326, 2011)**

To maintain normoglycemia, the pancreatic β-cell secretes insulin in response to a rise in blood glucose concentration. Concomitantly, glucose stimulates a rapid increase in proinsulin and secretory membrane protein synthesis, thereby ensuring the maintenance of secretory capacity (1–6). Because the endoplasmic reticulum (ER) is the site of synthesis of all secretory membrane proteins, glucose-dependent rises in the rate of secretory membrane protein synthesis places a huge demand on the pancreatic β-cell's ER protein folding, modification, and processing capacity. Conditions that disturb ER homeostasis can impact on ER protein folding and processing, resulting in the accumulation of malfolded protein within the lumen of the ER and ER stress (7, 8). To alleviate ER stress and promote cell survival, the cell activates a series of signal transduction cascades termed the unfolded protein response (UPR) that act to decrease ER protein folding load, increase ER protein folding capacity, and increase the clearance of malfolded proteins from the ER (9). The transducers of the UPR are three ER transmembrane proteins: the protein kinase R (PKR) like ER protein kinase (PERK), the activating transcription factor-6 (ATF6) and

ISSN Print 0888-8809 ISSN Online 1944-9917
Printed in U.S.A.

doi: 10.1210/me.2010-0309 Received August 2, 2010. Accepted December 2, 2010.
First Published Online December 30, 2010

Abbreviations: AMPK, AMP kinase; ATF, activating transcription factor; $[Ca^{2+}]_{ER}$, ER Ca^{2+} concentration; $[Ca^{2+}]_i$, intracellular Ca^{2+} concentration; CHOP-10, C/EBP homologous protein-10; CPA, cyclopiazonic acid; eIF2α, eukaryotic initiation factor 2α; ER, endoplasmic reticulum; FRET, fluorescence resonance energy transfer; GADD, growth-arrest and DNA damage-inducible protein; GFP, green fluorescent protein; IRE, inositol-requiring enzyme; ISR, integrated stress response; KRB, Krebs-Ringer bicarbonate buffer; PERK, protein kinase R like ER kinase; SERCA, sarcoplasmic/ER Ca^{2+}-ATPase; UPR, unfolded protein response; XB1, X-box transcription factor 1.

the inositol-requiring enzyme 1 (IRE1). Once activated, PERK phosphorylates the eukaryotic initiation factor-2 (eIF2) on serine 51 of its α-subunit, resulting in the repression of protein synthesis and the up-regulation of the expression of ATF4 (10, 11). PERK also phosphorylates and activates the transcription factor nuclear factor (erthyoid derived 2) (12). The increased expression and activation of ATF4 and nuclear factor (erythroid-derived 2), respectively, results in an increase in the expression of antiapoptotic proteins involved in maintaining redox homeostasis and combating oxidative stress (13). IRE1 is a ribonuclease that, when activated, splices the mRNA encoding X-box transcription factor 1 (XBP1), leading to a frame shift and the production of XBP1s, a larger more active form of this protein. XBP1s increases the expression of a range of mRNA, many of which are important in increasing ER folding capacity and efficiency, such as the chaperone Ig heavy chain binding protein (glucose-regulated protein 78) (14). Upon the induction of ER stress, ATF6 is transported from the ER to the Golgi where it is cleaved by the serine proteases 1 and 2 (SP1/2), releasing its cytosolic domain, which translocates to the nucleus where it has overlapping functions to that of XBP1 (15).

There is great deal of evidence demonstrating that PERK plays a critical role in β-cells (16, 17). Loss-of-function mutations within PERK result in a rare autosomal recessive disorder called Wolcott-Rallison syndrome characterized by permanent neonatal or early-infancy insulin-dependent diabetes caused by β-cell dysplasia (17). PERK-knockout mice display a similar phenotype and develop insulin-dependent diabetes as a result of β-cell dysplasia (16). β-Cell dysplasia is likely caused by the inability of PERK to phosphorylate eIF2α because homozygous eIF2α serine 51 to alanine (S51A) knock-in mice (which creates a nonphosphorylatable eIF2α) also shows severe β-cell deficiency (11). Furthermore, β-cell-specific conditional eIF2α Ser51Ala knock-in mice display unrestricted protein synthesis which leads to oxidative stress and ultimately a decrease in ER function resulting in β-cell death (18). Interestingly, we have previously shown that PERK is activated in response to a decrease in glucose concentration in the pancreatic β-cell line MIN6, independently of IRE1, and that this is mediated by a decrease in the energy status of the cell (19). The resulting PERK-dependent phosphorylation of eIF2α (1, 19) was shown to play an important role in suppressing proinsulin and global protein synthesis in MIN6 cells at low glucose concentration (19). However, the molecular mechanisms by which PERK is activated at low glucose concentration and its role in β-cell function are poorly understood.

In the present study, we provide evidence that a decrease in the energy status of the cell in response to a decrease in glucose concentration results in sarcoplasmic/ER Ca^{2+}-ATPase (SERCA) pump inhibition, which leads to a decreased rate of ER Ca^{2+} influx, resulting in ER Ca^{2+} depletion. This in turn leads to the activation of PERK. We also demonstrate that PERK-dependent eIF2α phosphorylation at low glucose suppresses proinsulin and global protein synthesis in rat islets of Langerhans, is essential for cell survival, and confers preemptive cytoprotection against ER stress in INS-1E cells.

Results

A decrease in extracellular glucose results in ER Ca^{2+} depletion and the activation of PERK

In the pancreatic β-cell line MIN6, a decrease in extracellular glucose concentration leads to the activation of PERK via an unknown mechanism (19). However, the ER requires a high luminal free ER Ca^{2+} concentration ($[Ca^{2+}]_{ER}$) to function efficiently, and alterations in $[Ca^{2+}]_{ER}$ can adversely affect the folding of newly synthesized proteins (20–23). Additionally, a number of reports link PERK activation with the lowering of ER Ca^{2+} (24). Therefore, it is conceivable that a decrease in glucose concentration may lead to the efflux of calcium from the ER and the activation of PERK. To investigate this possibility, we measured $[Ca^{2+}]_{ER}$ using the fluorescence resonance energy transfer (FRET)-based probe D1ER cameleon, which is targeted to the ER via a KDEL ER retention sequence (25). This probe contains a Ca^{2+}-binding domain that, once Ca^{2+} is bound, allows high efficiency of excitation transfer from the donor cyan fluorescent protein to the acceptor yellow fluorescent protein. The degree of FRET provides a ratiometric indicator of Ca^{2+} levels within the ER. MIN6 cells expressing D1ER cameleon were preincubated for 1 h in Krebs-Ringer bicarbonate buffer (KRB) at 20 mM glucose before perfusion with KRB containing 11.1, 5.5, or 0 mM glucose. The perfusion of KRB at 11.1, 5.5, or 0 mM glucose all led to a rapid glucose concentration-dependent decrease in $[Ca^{2+}]_{ER}$ (Fig. 1A). These decreases in $[Ca^{2+}]_{ER}$ paralleled an increase in the activation of PERK, as assessed using a phospho-specific antibody to Thr980 and by monitoring the phosphorylation of its substrate eIF2α on Ser51 (Fig. 1B). In addition, PERK is rapidly activated upon glucose deprivation (Fig. 1C), and the overexpression of a dominant-negative form of PERK (PERKΔC) confirmed our previous findings (19) that eIF2α phosphorylation in response to a decrease in glucose concentration is dependent upon PERK activation (Fig. 1D).

To investigate whether a decrease in glucose concentration also leads to ER Ca^{2+} store depletion and PERK-dependent eIF2α phosphorylation in primary β-cells, we

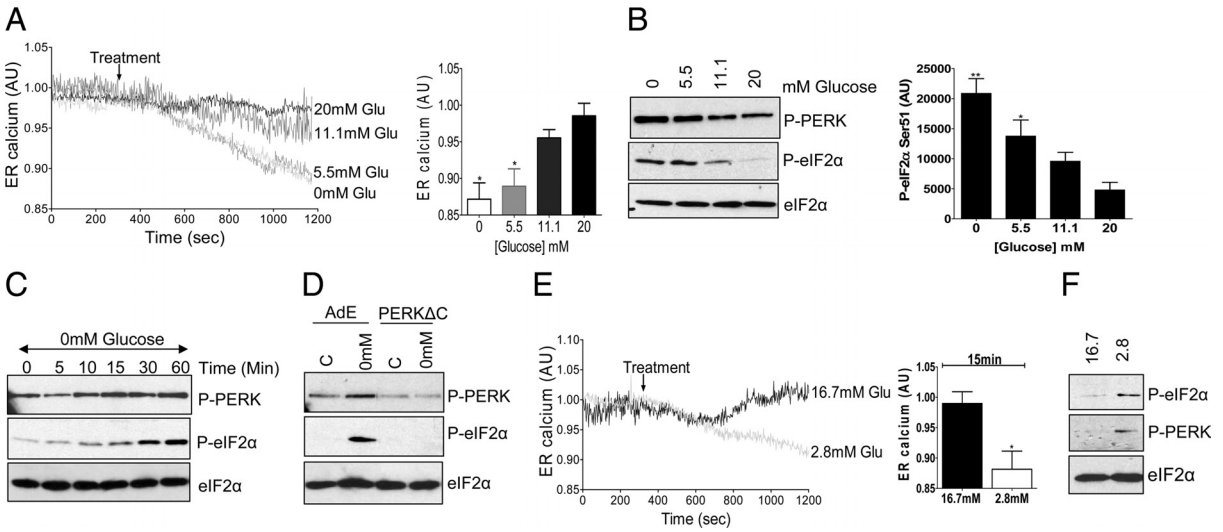

FIG. 1. Physiologically relevant decreases in glucose concentration causes $[Ca^{2+}]_{ER}$ depletion and PERK activation in MIN6 cells and islets of Langerhans. Panel A, $[Ca^{2+}]_{ER}$ was measured in intact MIN6 cells using the D1ER cameleon probe. Cells were incubated with KRB containing 20 mM glucose (Glu) before being incubated with KRB in the presence of 11.1, 5.5, or 0 mM glucose. Quantitative comparison of the $[Ca^{2+}]_{ER}$ levels compared with control (20 mM glucose). Results are from three separate experiments (five to 15 cells per experiment) shown as mean ± SEM; n = 3. *, $P < 0.05$. *P* value was obtained using a one-way ANOVA followed by Bonferroni posttests compared with control (20 mM glucose). Panel B, MIN6 cells were preincubated in KRB containing 20 mM glucose for 1 h. Cells were then treated with KRB supplemented with the indicated concentrations of glucose for 1 h. Proteins were resolved on SDS-PAGE and Western blotted using antisera against phospho-PERK (P-PERK) (Thr980), phospho-eIF2α (P-eIF2α) (Ser51), and total eIF2α as a loading control. Quantified Western blots of phospho-eIF2α are shown as mean ± SEM; n = 3.*, $P < 0.05$; **, $P < 0.01$. *P* value was obtained using a one-way ANOVA followed by Bonferroni posttests compared with control (20 mM glucose). Panel C, Time course of PERK activation. MIN6 cells were preincubated in KRB containing 20 mM glucose for 1 h. Cells were then treated with KRB in the absence of glucose for the times indicated in the figure. Proteins were resolved on SDS-PAGE and Western blotted using antisera against phospho-PERK (Thr980), phospho-eIF2α (Ser51), and total eIF2α as a loading control. Panel D, MIN6 cells were infected with Ad-Empty (AdE) or Ad-PERKΔC for 48 h. After infection, the cells were preincubated in KRB in the presence of 20 mM glucose for 1 h. Cells were then treated for an additional 1 h in KRB containing 20 mM glucose [control (C)] or in the absence of glucose (0 mM). Proteins were resolved on SDS-PAGE and Western blotted using antisera against phospho-PERK (Thr980), phospho-eIF2α (Ser51), and total eIF2α as a loading control. Panel E, $[Ca^{2+}]_{ER}$ was measured in dispersed islets using the D1ER cameleon probe. Cells were treated with KRB containing 16.7 mM glucose before being treated with KRB in the presence of 2.8 mM glucose. Quantitative comparison was made of the $[Ca^{2+}]_{ER}$ levels induced by glucose deprivation compared with control (16.7 mM glucose) and analyzed via Student's *t* test, unpaired and two tailed; *, $P < 0.05$ results are from three separate experiments (three to eight cells per experiment). Panel F, Islets were incubated at 2.8 or 16.7 mM glucose. Proteins were resolved on SDS-PAGE and Western blotted using antisera against phospho-PERK (Thr980), phospho-eIF2α (Ser51), and total eIF2α as a loading control.

measured changes in $[Ca^{2+}]_{ER}$ and PERK phosphorylation in dispersed rat islets. Incubation of dispersed islets at low glucose concentration resulted in a decrease in $[Ca^{2+}]_{ER}$, which paralleled the phosphorylation of PERK and its substrate eIF2α (Fig. 1, E and F).

In summary, physiologically relevant decreases in glucose concentration lead to a concentration-dependent decrease in $[Ca^{2+}]_{ER}$, which parallels increases in PERK activation in both MIN6 cells and islets of Langerhans.

SERCA pump activity is inhibited by a decrease in glucose concentration independently of changes in intracellular Ca^{2+} concentration ($[Ca^{2+}]_i$)

$[Ca^{2+}]_{ER}$ is maintained through calcium influx through SERCA (26). This is an energy-dependent process, and therefore, one possible mechanism for ER calcium depletion in response to glucose deprivation is via SERCA pump inhibition. To investigate whether ER calcium depletion and PERK-dependent eIF2α phosphorylation in response to a decrease in glucose concentration was likely mediated by SERCA pump inhibition, we measured SERCA pump activity at defined glucose concentrations. MIN6 cells were preincubated with 20 mM glucose for 1 h. During the last 15 min, the reversible SERCA pump inhibitor cyclopiazonic acid (CPA) (10 μM) was added to deplete ER calcium stores (Fig. 2A). The cells were then perfused with KRB containing 20, 11.1, 5.5, or 0 mM glucose and the rate of refilling of ER calcium stores determined (Fig. 2, A and B). In addition, the intracellular ATP concentration was quantified (Fig. 2C). The perfusion of cells with KRB containing 20 mM glucose led to the rapid refilling of the ER, indicating a high rate of SERCA pump activity (Fig. 2, A and B). In contrast, when cells were perfused with KRB minus glucose, no significant increase in Ca^{2+} reuptake into the ER was observed, indicating that glucose deprivation inhibits the SERCA pump (Fig. 2, A and B). Perfusion of cells with KRB plus 11.1 or 5.5 mM glucose led to a dose-dependent decrease in the rate of refilling and the maximal $[Ca^{2+}]_{ER}$ compared with cells incubated at 20 mM glucose (Fig. 2, A and

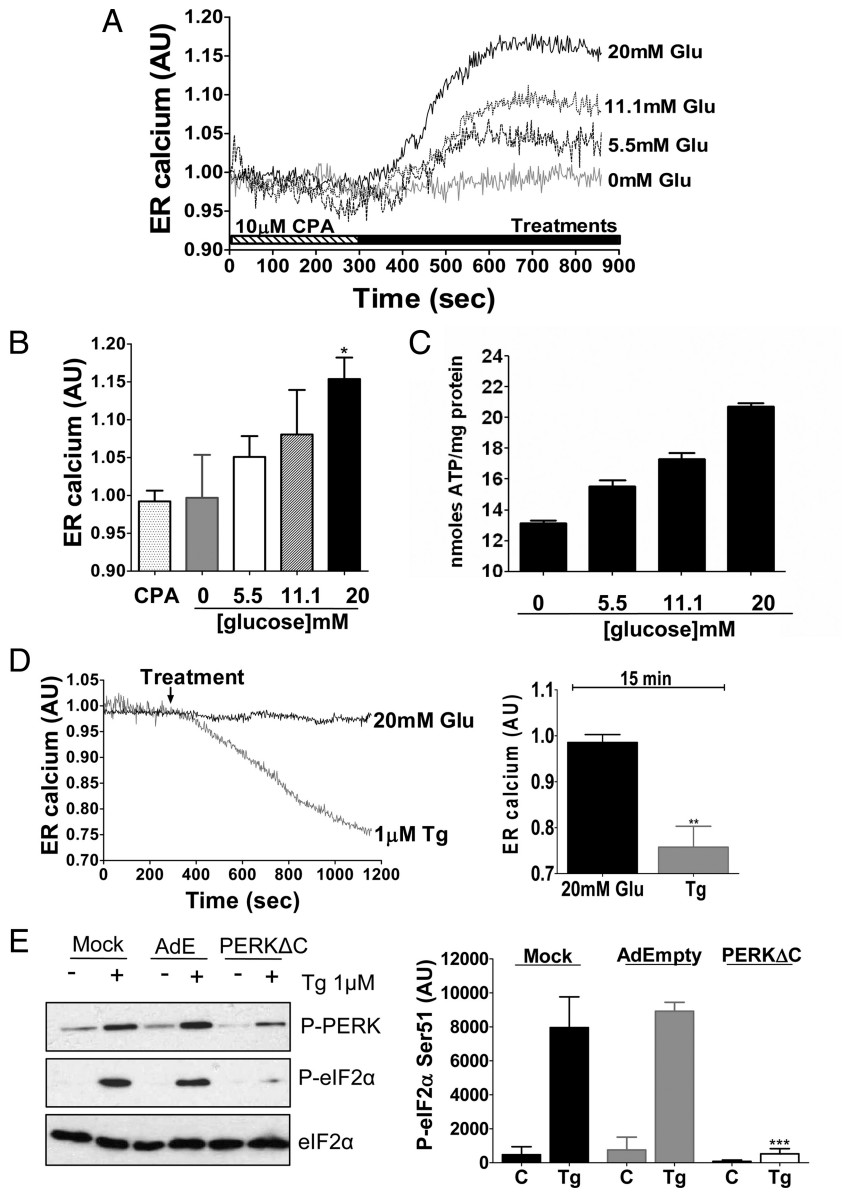

FIG. 2. SERCA is inhibited by a decrease in glucose concentration, and SERCA pump inhibition leads to PERK activation. Panel A, $[Ca^{2+}]_{ER}$ was measured in intact MIN6 cells using the D1ER cameleon probe. To monitor the rate of $[Ca^{2+}]_{ER}$ refilling, the ER store was depleted of Ca^{2+} by incubating cells in KRB containing 20 mM glucose and 10 μM CPA for 15 min. Cells were then perfused with KRB containing 0, 5.5, 11.1, and 20 mM glucose. Panel B, Quantitative comparison of the $[Ca^{2+}]_{ER}$ levels. Results are from three separate experiments (five to 15 cells per experiment) shown as mean ± SEM; n = 3.*, $P < 0.05$. *P* value was obtained using a one-way ANOVA followed by Bonferroni posttests compared with control (20 mM glucose). Panel C, MIN6 cells were incubated with KRB containing 20 mM glucose before being incubated with KRB in the presence of 11.1, 5.5, or 0 mM glucose for 15 min. ATP content is expressed as nanomoles of ATP per milligram of total protein shown as mean ± SEM; n = 3. $P < 0.0001$ as determined using one-way ANOVA. Panel D, $[Ca^{2+}]_{ER}$ was measured in intact MIN6 cells treated with 20 mM glucose in the presence or absence of 1 μM thapsigargin. Quantitative comparison of the $[Ca^{2+}]_{ER}$ levels induced by thapsigargin compared with control (20 mM glucose) are plotted ± SEM and analyzed via Student's *t* test, unpaired and two tailed; **, $P < 0.01$. Results are from three separate experiments (five to 15 cells per experiment). Panel E, MIN6 cells were mock-infected or infected with Ad-Empty (AdE) or Ad-PERKΔC for 48 h. After infection, the cells were preincubated in KRB in the presence of 20 mM glucose for 1 h. Cells were then treated for an additional 1 h in KRB in the presence or absence of 1 μM thapsigargin (Tg). Proteins were resolved on SDS-PAGE and Western blotted using antisera against phospho-PERK (P-PERK) (Thr980), phospho-eIF2α (P-eIF2α) (Ser51), and total eIF2α as a loading control. Quantified Western blots of phospho-eIF2α are shown as means ± SEM; n =3.***, $P < 0.001$. *P* value was obtained using a one-way ANOVA compared with control (Mock). AU, Arbitrary units; C, control.

B). Interestingly, a decrease in the rate of SERCA pump activity paralleled a decrease in the intracellular ATP concentration (Fig. 2, A–C). To confirm that SERCA pump inhibition *per se* can lead to ER calcium depletion and the activation of PERK in MIN6 cells, cells were incubated in KRB containing 20 mM glucose in the presence of the SERCA pump inhibitor thapsigargin (1 μM). As expected, thapsigargin induced a significant decrease in $[Ca^{2+}]_{ER}$ (Fig. 2D) and the phosphorylation of PERK and its downstream target eIF2α, which were inhibited in cells overexpressing a dominant-negative mutant of PERK (PERKΔC) (Fig. 2E).

A decrease in extracellular glucose concentration leads to a reduction in $[Ca^{2+}]_i$ (Fig. 3A). This could in turn cause, or potentiate, ER calcium store depletion through an increase in the ER to cytosol calcium concentration gradient. To investigate this possibility, we determined whether depolarizing concentration of KCl (K50), which evokes a large and sustained rise in intracellular Ca^{2+} (Fig. 3B), would inhibit the rate of ER calcium depletion in the absence of glucose. However, this had no effect on the rate or extent of $[Ca^{2+}]_{ER}$ depletion (Fig. 3C) in response to glucose deprivation. Therefore, a decrease in $[Ca^{2+}]_{ER}$ in response to a decrease in glucose concentration is independent of changes in $[Ca^{2+}]_i$.

A decrease in the energy status of the cell results in the depletion of ER calcium stores via inhibition of the SERCA pump

Our results provide evidence that SERCA pump inhibition by a decrease in glucose concentration leads to a decrease in $[Ca^{2+}]_{ER}$ and a marked increase in the phosphorylation of eIF2α via a PERK-dependent mechanism (Figs. 1 and 2).We had previously shown that a decrease in extracellular glucose concentration resulted in a fall in the intracellular energy status that paralleled increases in PERK-depen-

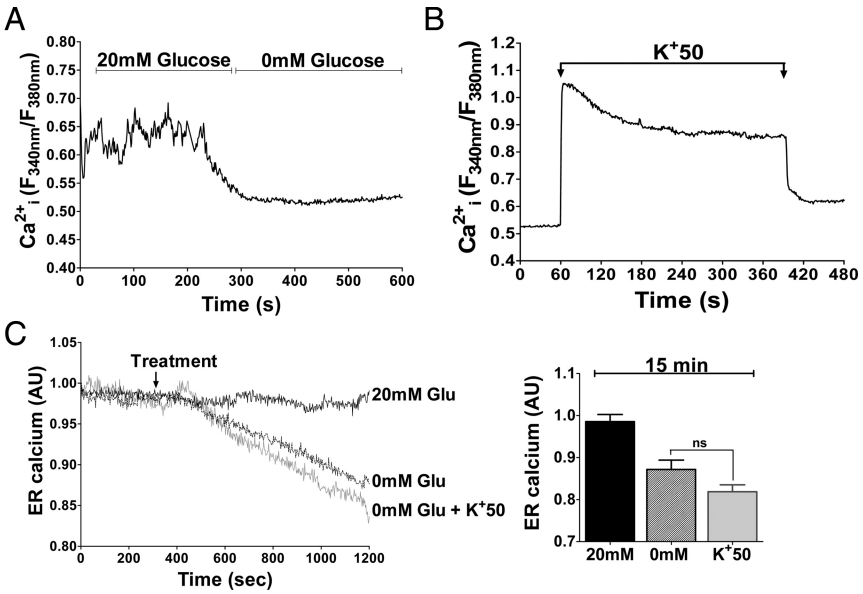

FIG. 3. The ER to cytosolic calcium concentration gradient does not influence ER calcium store depletion in glucose-deprived cells. A and B, $[Ca^{2+}]_i$ was measured using fura-2-AM. MIN6 cells were exposed to 20 mM glucose and then 0 mM glucose (A) or 0 mM glucose plus depolarizing concentrations of potassium (K^+50) (B). Representative traces are shown. Results are from three separate experiments (20–30 cells per experiment). C, $[Ca^{2+}]_{ER}$ was measured using the D1ER cameleon probe in response to depolarizing concentrations of potassium (K^+50). Quantitative comparison was made of the $[Ca^{2+}]_{ER}$ levels induced by 0 mM glucose with or without K^+50. Results are from three separate experiments (five to 15 cells per experiment) shown as mean ± SEM; n = 3. Statistical analysis was performed using a one-way ANOVA followed by Bonferroni posttests between 0 mM and K^+50. AU, Arbitrary units.

dent eIF2α phosphorylation (19), and in this report, we show that a decrease in SERCA pump activity correlates with a decrease in intracellular ATP concentration (Fig. 2). Therefore, we wished to determine whether inhibition of the SERCA pump in response to a decrease in glucose concentration could be evoked by a decrease in energy status. To investigate this possibility, MIN6 cells were treated with a dose of oligomycin (12 nM), which leads to a reduction in intracellular [ATP] to a level similar to that found in MIN6 cells deprived of glucose for 1 h (19) (Fig. 4B). This resulted in a decrease in $[Ca^{2+}]_{ER}$ at a similar rate and to a similar extent to that observed upon glucose deprivation (Fig. 4A). Treatment of MIN6 cells with 12 nM oligomycin also led to a time-dependent increase in the activation of PERK and the phosphorylation of eIF2α, which paralleled decreases in the energy status of the cell, as assessed by the phosphorylation state of AMP-kinase (AMPK) [a sensor of intracellular AMP and hence cellular energy status (27)] (Fig. 4C). To determine whether 12 nM oligomycin also inhibits SERCA pump activity, cells were depleted of ER calcium and the rate of ER store refilling at 20 mM glucose was determined in the presence or absence of oligomycin. Oligomycin (12 nM), like glucose deprivation, also inhibited ER Ca^{2+} store refilling (Fig. 4D). In conclusion, oligomycin, at a concentration of 12 nM that depletes intracellular [ATP] to a similar level to that found in glucose-deprived cells, inhibits SERCA pump activity and causes ER Ca^{2+} depletion (Fig. 4) and PERK-dependent phosphorylation of eIF2α (19).

A decrease in extracellular glucose concentration causes PERK-dependent inhibition of proinsulin and global protein synthesis in rat islets of Langerhans

Having established the molecular mechanism of eIF2α phosphorylation at low glucose concentration, we wished to determine its physiological role in islets. To investigate whether eIF2α phosphorylation at low glucose influences protein synthesis in islets, we monitored changes in proinsulin and total protein synthesis in dispersed rat islets infected with an N-terminal truncation mutant of growth-arrest and DNA-damage-inducible protein 34 (GADD34), GADD34ΔN, which constitutively directs protein phosphatase-1 to eIF2α, leading to eIF2α dephosphorylation (28) and as control an empty adenovirus (Ad-Empty). At 48 h after infection, the cells were incubated at 2.8 or 16.7 mM glucose, and the phosphorylation status of eIF2α was assessed by Western blotting (Fig. 5). Incubating the Ad-Empty control cells at low glucose (2.8 mM) resulted in an increase in the phosphorylation of eIF2α that was inhibited in cells overexpressing GADD34ΔN (Fig. 5A). Importantly, the overexpression of GADD34ΔN also resulted in a significant increase in proinsulin and global protein synthesis at low glucose (Fig. 5B). In addition, we investigated changes in the levels of translational ternary complex formation *in vivo* (1, 29). Dispersed islets were infected with recombinant adenovirus encoding luciferase downstream of the 5′-untranslated region of ATF4 and, as internal control, green fluorescent protein (GFP), both under the control of a cytomegalovirus promoter (Ad-ATF4Luc) (1). ATF4 translation is regulated by short open reading frames in its 5′-untranslated region by a mechanism analogous to that which regulates *GCN4* expression in yeast (30, 31). Briefly, upon an increase in ternary complex availability, ATF4 expression is repressed. However, when the availability of ternary complex is low, ATF4 expression is up-regulated (30, 31). Incubation of cells at low glucose led to an increase in luciferase/GFP ratio (Fig. 5C) that paralleled eIF2α phosphorylation (Fig. 5A), indicating a decrease in ternary

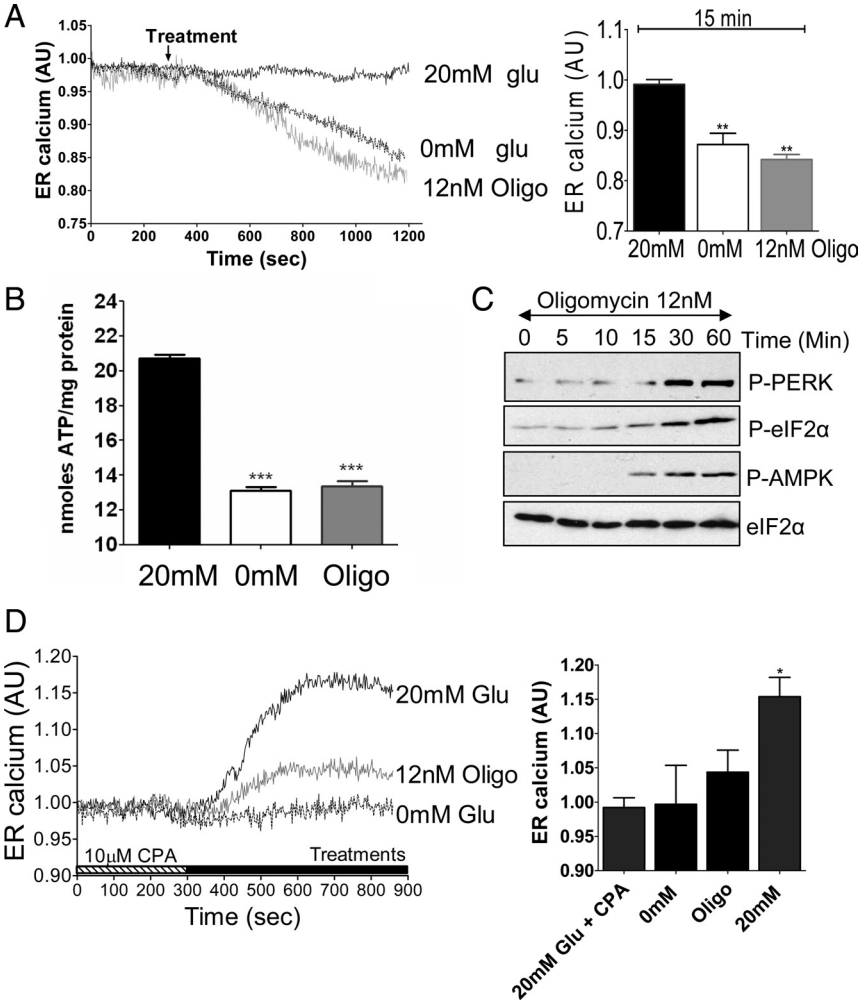

FIG. 4. A decrease in the energy status of the cell results in the depletion of ER calcium stores via inhibition of the SERCA pump. A, $[Ca^{2+}]_{ER}$ was measured in intact MIN6 cells using the D1ER cameleon probe. Cells were treated with KRB containing 20 mM glucose (glu) before being treated with KRB supplemented with 20 mM glucose in the presence of 12 nM oligomycin (Oligo) or KRB minus glucose. Quantitative comparison of the $[Ca^{2+}]_{ER}$ levels compared with control (20 mM glucose). Results are from three separate experiments (five to 15 cells per experiment) shown as mean ± SEM; n = 3. **, $P < 0.01$. *P* value was obtained using a one-way ANOVA followed by Bonferroni posttests compared with control (20 mM glucose). B, MIN6 cells were incubated with KRB containing 20 mM glucose before being treated with 12 nM oligomycin or incubated with KRB minus glucose for 15 min. ATP content is expressed as nanomoles of ATP per milligram of total protein shown as mean ± SEM; n = 3. ***, $P < 0.005$. *P* value was obtained using a one-way ANOVA followed by Bonferroni posttests compared with control (20 mM glucose). C, MIN6 cells were preincubated in KRB containing 20 mM glucose for 1 h. Cells were then treated with KRB supplemented with 20 mM glucose in the presence of 12 nM oligomycin for the times indicated. Proteins were resolved on SDS-PAGE and Western blotted using antisera against phospho-PERK (P-PERK) (Thr980), phospho-eIF2α (P-eIF2α) (Ser51), phospho-AMPK (P-AMPK) (Thr172), and total eIF2α as a loading control. Results are representative of three separate experiments. D, To monitor the rate of $[Ca^{2+}]_{ER}$ refilling, the ER store was depleted of Ca^{2+} by incubating cells in KRB containing 20 mM glucose and 10 μM CPA for 15 min. Cells were then perfused with KRB containing 12 nM oligomycin in the presence of 20 mM glucose or as controls KRB or KRB 20 mM glucose. Quantitative comparison was made of the $[Ca^{2+}]_{ER}$ levels. Results are from three separate experiments (five to 15 cells per experiment) shown as mean ± SEM; n = 3. *, $P < 0.05$. *P* value was obtained using a one-way ANOVA followed by Bonferroni posttests compared with control (20 mM glucose plus CPA).

complex formation, a prerequisite for the up-regulation of ATF4 and induction of the integrated stress response (ISR), a response that in other cell types can influence cell viability and confer cytoprotection (32). In conclusion, PERK activation at low glucose concentration decreases ternary complex formation and suppresses proinsulin and global protein synthesis in islets.

eIF2α phosphorylation plays an important role in maintaining β-cell viability and confers preemptive cytoprotection

Because eIF2α phosphorylation has been shown to play an important role in pancreatic β-cell survival, we investigated whether changes in eIF2α phosphorylation in response to glucose impacted on pancreatic β-cell viability. Extended incubation of the rat pancreatic β-cell line INS-1E with decreasing glucose concentrations led to an increase in the phosphorylation of eIF2α (Fig. 6A) and a decrease in cell viability at 2.8 mM glucose (as determined as the percentage of cells within the sub-G1/0 population as assessed using flow cytometry) (Fig. 6B). However, the expression of GADD34ΔN, which effectively blocked eIF2α phosphorylation (Fig. 6A), caused a further decrease in cell viability at low glucose, which is significant at 5.5 mM, indicating that in these cells, eIF2α phosphorylation is important in maintaining β-cell viability at physiologically low glucose concentration (Fig. 6, A and B).

The ISR is cytoprotective in other cell types, and therefore, PERK-dependent activation of the ISR evoked at physiologically relevant low glucose concentrations, such as during periods of fast, may protect β-cells from subsequent oxidative and/or ER stress that occurs in response to a rise in blood glucose concentration (33, 34). To investigate whether eIF2α phosphorylation confers resistance to ER stress, INS-1E cells were pretreated with CPA or incubated in the absence of glucose to cause PERK-dependent eIF2α phosphorylation (Fig. 6, C–E). The absence of glucose led to an ISR as determined by an increase in eIF2α phosphorylation and an increase in ATF4 and

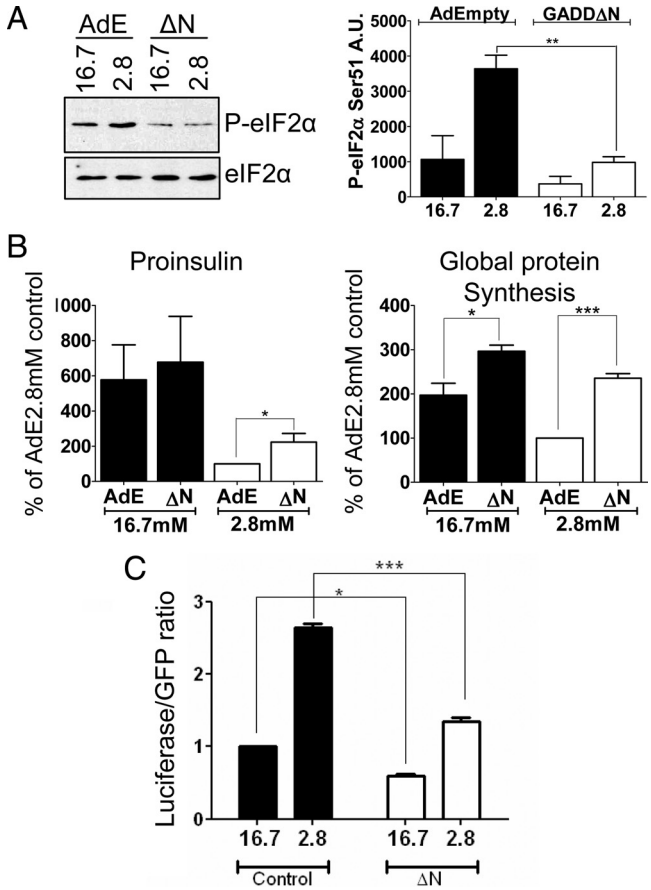

FIG. 5. Functional consequences of PERK activation on protein synthesis in rat islets of Langerhans. A, Dispersed islets were infected with control Ad-Empty virus (AdE) or AdGADDΔN (ΔN) for 48 h. After infection, the cells were incubated for 2 h in KRB at 2.8 or 16.7 mM glucose in the presence of ^{35}S-labeled methionine/cysteine. Proteins were resolved on SDS-PAGE and Western blotted using antisera against phospho-eIF2α (P-eIF2α) (Ser51) or total eIF2α as a loading control. Quantified Western blots of phospho-eIF2α are shown as mean ± SEM; n = 3. **, $P < 0.01$. P value was obtained using a one-way ANOVA followed by Bonferroni posttests. B, Densitometry values from autoradiographs of ^{35}S-labeled methionine/cysteine incorporation into proinsulin and total protein are plotted ± SEM and analyzed by Student's t test, unpaired and two tailed; *, $P < 0.05$; **, $P < 0.01$; ***, $P < 0.005$ (n = 3) expressed as a percentage of 2.8 mM (Ad-Empty). C, Dispersed islets were infected with Ad-ATF4luc in the presence or absence of Ad-GADDΔN for 24 h. After infection, the cells were incubated for 2 h in KRB at 2.8 or 16.7 mM glucose in the presence of ^{35}S-labeled methionine/cysteine. Cells were then lysed, and luciferase and GFP were immunoprecipitated. Immunoprecipitants were run out on SDS-PAGE gels, and the incorporation of [^{35}S]methionine/cysteine into luciferase and GFP were detected by autoradiography and expressed as luciferase/GFP ratio.

C/EBP homologous protein (CHOP) 10 expression (Fig. 6F). The cells were then allowed to recover for 24 h before exposure to the ER stress agent thapsigargin. Recovery did not result in an increase in $[Ca^{2+}]_{ER}$ compared with untreated cells (Fig. 6E). Crucially, pretreatment with either CPA or preincubation in glucose-free media offered a significant protection against ER-stress-induced cell death (Fig. 6, B and C). This protection also correlated with a decrease in the phosphorylation status of eIF2α upon thapsigargin treatment (Fig. 6F). Importantly, the overexpression of GADD34ΔN blocked the protective effect induced by low glucose pretreatment (Fig. 6G). Taken together, these results provide evidence that incubation of INS-1E cells at low glucose confers cytoprotection against subsequent ER stress and that this is dependent upon the phosphorylation of eIF2α.

Discussion

In pancreatic β-cells, a rise in extracellular glucose concentration causes an initial reduction in ER-sequestered Ca^{2+}, which is rapidly followed by a large increase in ER Ca^{2+} uptake into an inositol triphosphate-sensitive Ca^{2+} pool (35–38). In this report, we show in both MIN6 cells and islets of Langerhans that a decrease in extracellular glucose concentration promotes a decrease in $[Ca^{2+}]_{ER}$ (Figs. 1 and 2). We also show that the treatment of MIN6 cells with oligomycin, at a concentration that reduces [ATP]/energy status of the cell to that found in glucose-deprived cells, also promotes a decrease in $[Ca^{2+}]_{ER}$ (Fig. 4). This is in agreement with a previous report demonstrating that carbonyl cyanide *m*-chloro-phenyl hydrazone, which dissipates the mitochondrial membrane potential and thereby inhibits ATP production, decrease $[Ca^{2+}]_{ER}$ in INS-1E cells (35). We provide evidence that the effects of a decrease in glucose concentration and/or a decrease in [ATP]/energy status on ER calcium store depletion is mediated by a reduction in SERCA pump activity (Figs. 1 and 2). Indeed, agents such as thapsigargin and CPA, which inhibit the SERCA pump and deplete ER calcium, also lead to the activation of PERK in pancreatic β-cells (Fig. 2) (7, 24). Therefore, we conclude that a decrease in glucose concentration results in a decrease in the energy status of the cell, which in turn results in ER Ca^{2+} store depletion through SERCA pump inhibition. However, studies on permeabilized β-cells indicate half-maximal Ca^{2+} uptake ranges from 3.5–45 nM ATP depending on $[Ca^{2+}]_i$ (36). Yet, we and others have provided evidence in intact β-cells that SERCA pump activity is regulated by physiological changes in glucose concentration (this report and Ref. 36) despite cytoplasmic ATP concentration varying within the millimolar range (36, 39). However, *K*ATP channels in pancreatic β-cells are half-maximally inhibited when excised membrane patches are exposed to 10–15 mM ATP yet respond to physiological changes in glucose concentration (39). In this case, the *K*ATP channel's sensitivity to ATP is reduced by phosphatidylinositol-4,5-bisphosphate and related phosphoinositides, long-chain acyl-coenzyme A esters, and MgADP. This allows the *K*ATP channel to be

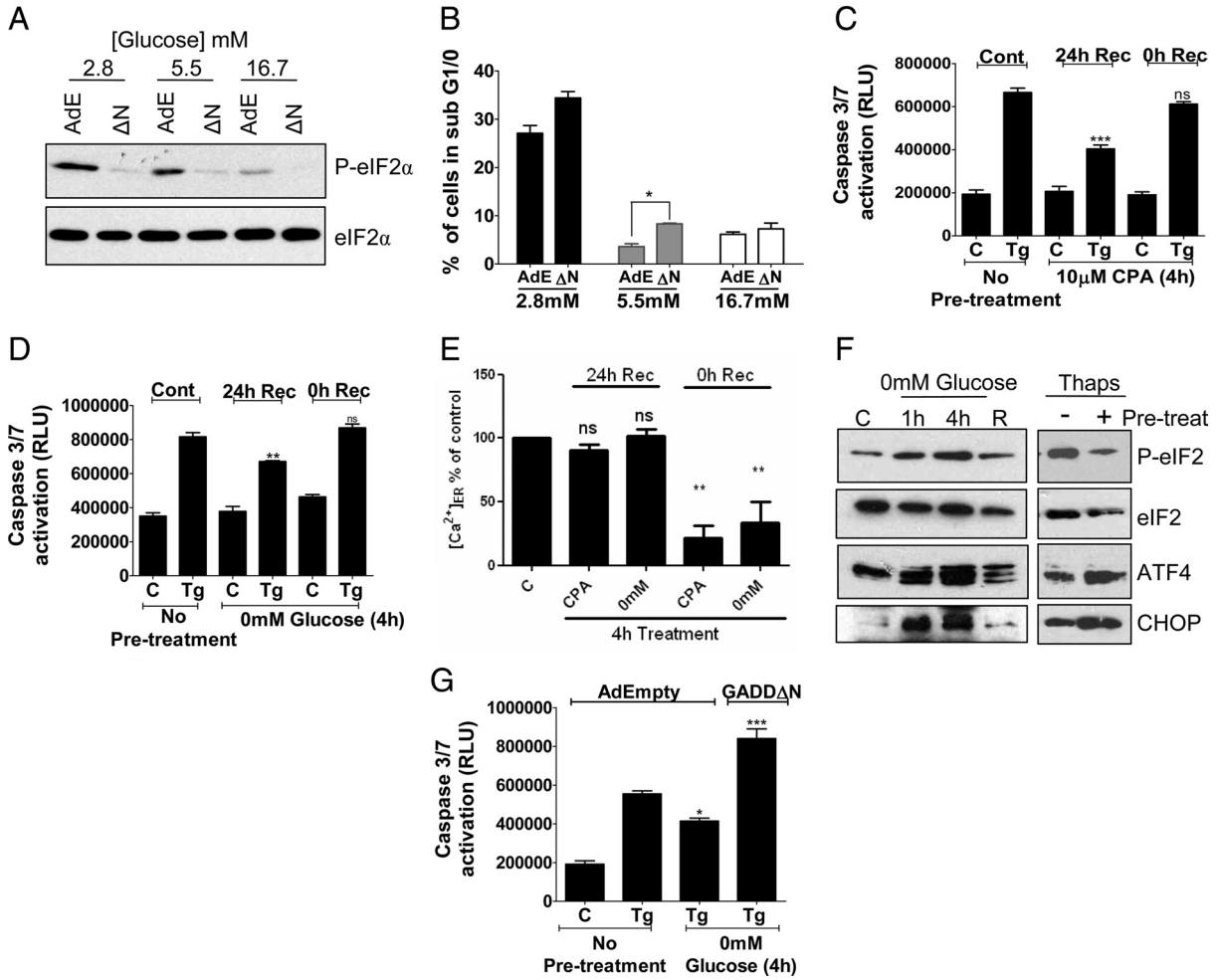

FIG. 6. PERK-dependent eIF2α phosphorylation plays an important role in maintaining β-cell viability and confers preemptive cytoprotection against ER stress. INS-1E cells were infected with control Ad-Empty (AdE) or AdGADDΔN (ΔN) viruses and incubated in full DMEM minus glucose medium supplemented with 2.8, 5.5, or 16.7 mM glucose for 48 h. Panels A and B, Cells were then lysed and proteins resolved on SDS-PAGE and Western blotted using antisera against phospho-eIF2α (P-eIF2α) (Ser51) or total eIF2α as a loading control (A) fixed and propidium iodide stained for analysis by flow cytometry (B). The percentage of dead cells was determined by the percentage of cells within the sub $G_{1/0}$ population. Results were analyzed by an unpaired and two-tailed Student's *t* test; *, $P < 0.05$ (n = 4). Panels C and D, Survival of INS-1E cells pretreated for 4 h with either 10 μM CPA (C) or 0 mM glucose (D) followed by 24 h of recovery and subsequent challenge with 1 μM thapsigargin (Tg) for 8 h. Panel E, INS-1E cells were treated for 4 h with either 10 μM CPA or incubated in RPMI minus glucose followed by 24 h of recovery (24 h Rec) or not (0 h Rec). Cells were loaded with 2 μM Fluo4 in KRB minus calcium before injection of 10 μM ionomycin. Changes in fluorescence were read immediately in a Novostar (BMG Labtech) 96-well plate reader. Peak increases in calcium upon ionomycin treatment were measured and plotted as percentage of control. Panel F, Cytoplasmic and nuclear extracts were collected from untreated INS-1E cells or cells incubated with 0 mM glucose for 1 and 4 h, 24 h after recovery (R) and after 8 h exposure to thapsigargin. Proteins were resolved on SDS-PAGE and Western blotted using antisera against phospho-eIF2α (Ser51), ATF-4, CHOP, and total eIF2α as a loading control. Panel G, INS-1E cells were infected with a control Ad-Empty virus or infected with AdGADDΔN for 36 h. After infection, the cells were incubated in the absence of glucose for 4 h followed by 24 h recovery and subsequent challenge with 1 μM thapsigargin for 8 h. In panels C, D, and G, cells were subjected to a luminometric caspase 3/7 activation assay as described in *Materials and Methods*. Data are expressed as relative light units (RLU). Results are expressed as mean ± SEM. *, $P < 0.05$; **, $P < 0.01$; ***, $P < 0.005$ (n = 6). *P* value was obtained using a one-way ANOVA followed by Bonferroni posttests compared with control (C).

regulated by changes in the ATP/ADP ratio in response to physiological changes in glucose concentration. Therefore, one possibility is that SERCA channel sensitivity to ATP is lowered by a yet undiscovered cytoplasmic factor. Alternatively, local changes in $[ATP]_i$ at the ER are much greater than global cytosolic changes in [ATP]. Interestingly, high concentrations of ADP have been reported to cause calcium leak through SERCA in muscle (40–42). Therefore, another intriguing possibility is that a decrease in glucose concentration increases [ADP], which in turn causes calcium leak through SERCA. It has been reported that ER calcium depletion inhibits glycoprotein processing, ER-associated degradation, and chaperone function, resulting in an accumulation of unfolded proteins within the ER, which in turn activates PERK as part of the UPR (for review see Ref. 43). Yet, we have previously provided evidence that glucose deprivation may lead to the activation of PERK via a mechanism that is independent of the accumulation of nascent unfolded proteins within the ER (19). However, this is technically difficult to confirm. In

addition, and in contrast to thapsigargin, glucose deprivation does not lead to IRE1 activation. However, the extent of ER Ca^{2+} store depletion is likely an important determinant as to which transducers of the UPR are activated. It is possible that the threshold for IRE1 activation in response to a decrease in $[Ca^{2+}]_{ER}$ is higher than that of PERK and is therefore activated in response to thapsigargin and not glucose deprivation.

PERK-dependent eIF2α phosphorylation clearly plays an important physiological function in islets of Langerhans as we show that the levels of total and proinsulin synthesis are significantly elevated at low glucose concentration in the absence of eIF2α phosphorylation (Fig. 5). However, the rate of proinsulin synthesis does not reach the levels observed at 16.7 mM glucose, indicating that additional specific mechanisms are in operation. These results concur with previous findings in MIN6 cells (19) and results obtained from β-cell-specific homozygous Ser51Ala conditional knock-in mice (18) in which the rate of both global and proinsulin biosynthesis were also significantly increased at low glucose concentrations in islets from these mice (18). eIF2α phosphorylation not only is important in repressing protein synthesis but can also increase the rate of translation of a small subset of mRNAs through a decrease in the availability of the translational ternary complex. These proteins whose expression is increased through both translational and transcriptional mechanisms form part of a well characterized response to eIF2α phosphorylation referred to as the ISR (29). The ISR is activated in both MIN6 cells and islets at low glucose concentrations (44, 45), and this response has been shown to be cytoprotective in other cell types (32). Interestingly, we show that eIF2α phosphorylation is important in maintaining β-cell viability (Fig. 6) and importantly that incubation of INS-1E cells at low glucose activates the ISR and confers cytoprotection against subsequent ER stress and that this is dependent upon the phosphorylation of eIF2α (Fig. 6). Therefore, perhaps PERK-dependent eIF2α phosphorylation, evoked during periods of fasting, protects β-cells from subsequent oxidative and ER stress, which has been reported to occur in β-cells in response to high glucose concentration (46). In support of this, increased oxidative stress has been observed in islets from β-cell-specific homozygous Ser51Ala conditional knock-in mice, and this is thought to ultimately lead to β-cell dysfunction and death (18).

In summary, we provide evidence that a decrease in the ATP/energy status of the cell in response to a decrease in glucose concentration results in SERCA pump inhibition, the efflux of Ca^{2+} from the ER, and the activation of PERK, which plays an important role in both pancreatic β-cell function and survival.

Materials and Methods

Chemicals

Fetal calf serum (FCS) was purchased from Invitrogen (Carlsbad, CA). All other chemicals were obtained from Sigma Chemical Co. (St. Louis, MO), unless otherwise stated.

MIN6 and INS-1E cell culture and treatment

In this study, MIN6 cells (kindly provided by Prof. Jun-Ichi Miyazaki) were used between passages 25 and 40 at approximately 80% confluence. MIN6 cells were grown in DMEM containing 25 mM glucose supplemented with 15% heat-inactivated FCS, 100 μg/ml streptomycin, 100 U/ml penicillin sulfate, and 75 μM β-mercaptoethanol (*i.e.* complete medium), equilibrated with 5% CO_2, 95% air at 37 C. In this study, INS-1E cells (47) were used between passages 60 and 75 at approximately 80% confluence. INS-1E cells were grown in RPMI 1640 containing 11.1 mM glucose, 1 mM sodium pyruvate, 10 mM HEPES supplemented with 5% FCS, 100 μg/ml streptomycin, 100 U/ml penicillin sulfate, and 55 μM β-mercaptoethanol (*i.e.* complete medium), equilibrated with 5% CO_2, 95% air at 37 C. Before treatment, the medium was removed and the cells washed twice with HEPES-balanced KRB [115 mM NaCl, 5 mM KCl, 10 mM $NaHCO_3$, 2.5 mM $MgCl_2$, 2.5 mM $CaCl_2$, 20 mM HEPES (pH 7.4)] containing 0.5% BSA. Full details of treatments are provided in the figure legends. All treatments were stopped by the addition of ice-cold lysis buffer containing 1% Triton, 10 mM β-glycerophosphate, 50 mM Tris-HCl (pH 7.5), 1 mM EDTA, 1 mM EGTA, 1 mM sodium orthovanadate, 1 mM benzamidine HCl, 0.2 mM phenylmethylsulfonyl fluoride, 1 μg/ml each of leupeptin and pepstatin, 0.1% β-mercaptoethanol, and 50 mM sodium fluoride. The lysates were then centrifuged for 10 min at 16,000 $\times$ *g* at 4 C. The supernatants were kept, and total protein concentrations were determined by the Bradford assay (Bio-Rad, Hercules, CA) using BSA as standard. The protein lysates were stored at −80 C until further analysis.

Islet isolation and culture

Pancreatic islets were isolated from 200- to 250-g male Wistar rats by collagenase digestion and Histopaque density gradient centrifugation by a modification of the method of Guest *et al.* (2). Briefly, the pancreas was inflated by injecting 6 ml medium (RPMI 1640 medium containing 11.1 mM glucose) (Invitrogen) containing 1 mg/ml collagenase (Serva, Heidelberg, Germany) through the common pancreatic duct. The excised pancreata were then incubated at 37 C for 17 min. After incubation, the pancreata were then individually hand shaken for 1 min. The partially disaggregated tissue was then centrifuged for 3 min at 200 $\times$ *g* at 4 C. The pelleted material was then resuspended in RPMI 1640 and subjected to another cycle of resuspension and centrifugation. The pelleted material was then resuspended in RPMI containing 5% FCS and then filtered through a sieve. Each filtrate was centrifuged for 3 min at 200 $\times$ *g* at 4 C, and the pellets were resuspended in 10 ml Histopaque 1077 (Sigma) and over-layered with 10 ml RPMI 1640. The tubes were centrifuged for 20 min at 1600 $\times$ *g* at 4 C, and islets were recovered from the RPMI/Histopaque-1077 interface and washed once in RPMI containing 5% FCS. The islets were then hand-picked under a stereomicroscope. The islets were then cultured at 37 C in 5% CO_2, 95% air in RPMI 1640 medium containing 11.1 mM glucose and 5% FCS. Where indicated, islets were dispersed by incubation in Ca^{2+}-free solution (138

mM NaCl, 5.6 mM KCl, 1.2 mM $MgCl_2$, 5 mM HEPES, and 1 mM EGTA) for 10 min followed by gentle pipetting. Dispersed islets were cultured for up to 1 wk at 37 C in the presence of 5% CO_2 in serum-free RPMI 1640 containing 11.1 mM glucose, 5 g/liter BSA, 100 U/ml penicillin sulfate, and 100 μg/ml streptomycin before treatments described in the figure legends. Cells were lysed by the addition of sample loading buffer.

Adenoviral construction and infection

The generation of recombinant adenoviruses expressing amino acids 1–583 of PERK [*i.e.* dominant-negative PERK (Ad-PERKΔC)], an N-terminal truncation mutant of GADD34 that constitutively directs protein phosphatase-1 to eIF2α, leading to eIF2α dephosphorylation (Ad-GADDΔN), Ad ATF4-Luc (1) and GFP (Ad-Empty) have been previously described (1, 19). For infection, MIN6 cells were incubated in the presence of the virus for 48 h before treatments. Under these conditions, more than 90% of cells were infected as determined by monitoring enhanced GFP expression by fluorescence microscopy.

Protein synthesis measurements

Briefly, cells were incubated in the presence of [^{35}S]methionine/cysteine for 2 h. The cells were then lysed (as described in *MIN6 and INS-1E cell culture and treatment* and *Islet isolation and culture*), and equal amounts of protein were resolved on SDS-PAGE and visualized by autoradiography. Changes in [^{35}S]methionine/cysteine incorporation into protein were determined by densitometry.

Survival assays

INS-1E cells were plated on a 24-well plate and cultured in RPMI 1640 for 48 h. After pretreatment with media containing 0 mM glucose for 4 h, INS-1E cells were maintained in normal medium for the duration of recovery (24 h). After the recovery period, the medium was replaced with fresh medium containing 1 μM thapsigargin for 8 h. After 8 h of thapsigargin treatment, cellular apoptosis was determined by measurement of caspases 3 and 7 activity using the luminometric Caspase-Glo 3/7 assay (Promega, Madison, WI) according to the manufacturer's protocol using a NOVOstar microplate reader (BMG LabTechnologies, Offenburg, Germany).

SDS-PAGE and immunoblotting

SDS-PAGE and Western blotting were performed as described previously (1). Anti-phospho-eIF2α (Ser51) antibody was purchased from Biosource (Camarillo, CA). Anti-phospho-PERK (Thr980) and anti-phospho-AMPK (Thr172) antibodies were purchased from Cell Signaling Technology (Beverly, MA). Anti-eIF2α CHOP and ATF4 antibodies were purchased from Santa Cruz Biotechnology (Santa Cruz, CA). Detection was by horseradish peroxidase-linked antirabbit secondary antibodies and enhanced chemiluminescence (GE Healthcare, Piscataway, NJ).

Single-cell imaging with ER-targeted cameleon

Dispersed rat islets or MIN6 cells were cultured on poly-D-lysine-coated circular glass coverslips (28 mm) for 24 or 48 h, respectively. Cells were then transfected with 4 μg plasmid per coverslip, encoding the FRET-based ER-targeted cameleon D1ER (gift from Professor Roger Tsien, University of California) (25) and/or RFP-calreticulin (Clontech, Palo Alto, CA) using Lipofectamine 2000 (Invitrogen) as per the manufacturer's instructions. After 6 h, the medium was replaced with complete medium and cultured for an additional 48 h before experiments. Single-cell imaging was performed in HEPES-balanced KRB via standard epifluorescence microscopy. Cells were perfused at a constant rate of 3–5 ml/min with KRB at 37 C. Full details of treatments are provided in the figure legends. Cells were imaged on a Zeiss Axiovert 200 microscope (×40 magnification) (Carl Zeiss Microimaging, Inc., Hertfordshire, UK) using a MicroMax digital camera (Roper-Princeton Instruments, Trenton, NJ) controlled by MetaFluor software (Universal Imaging Corp., Downington, PA). Emission ratio imaging of the cameleon was achieved by using a 436DF20 excitation filter, a 450-nm dichroic mirror, and two emission filters: 475/40nm for enhanced GFP and 535/25nm for cyan fluorescent protein.

Quantification of cell death using flow cytometry

MIN6 or INS-1E cells were trypsinized off the plate and resuspended in full medium. The cells were then gently spun down, washed in PBS, and resuspended in 1 vol of PBS. To fix the cells, 9 vol of ice-cold methanol was added to the cells drop wise. The cells were then left for 18 h at −20 C. The cells were then spun down and resuspended in PBS containing 10 mg/ml propidium iodide and RNase A and incubated at room temperature for 30 min before analysis by flow cytometry using a FACSCalibur (Becton Dickinson, San Jose, CA).

Determination of cellular ATP content

ATP content was determined using a bioluminescent assay (Sigma) following the manufacturer's instructions. Briefly, after treatments, as described above and in the figure legends, cells were lysed by the addition of somatic-cell ATP-releasing reagent. Luminescence was then read immediately in a Novostar (BMG Labtech) 96-well plate reader with injectors.

Quantification of ER calcium stores using Fluo4

Quantification of ER calcium stores using Fluo4 was determined as described by Purkiss and Willars (48) with modifications. Cells were loaded at room temperature for 30 min with 2 μM Fluo4 in KRB minus calcium containing 0.02% pluronic acid and 2.5 mM probenecid. The cells were then washed twice in KRB minus calcium before injection of 10 μM ionomycin. Changes in fluorescence were read immediately in a Novostar (BMG Labtech) 96-well plate reader with injectors. Peak increases in calcium upon ionomycin treatment were measured and plotted as percentage of control.

Acknowledgments

We thank Dr. Ken Young and Roger Snowden from the Medical Research Council Toxicology Unit, Leicester, and Neil Johnston from the Department of Cell Physiology and Pharmacology, Leicester, for providing excellent technical advice and assistance. We also thank Professor Roger Y. Tsien for generously providing the cameleon D1ER construct.

Address all correspondence and requests for reprints to: Dr. T. P. Herbert, Department of Cell Physiology and Pharmacology, University of Leicester, The Henry Wellcome Building, University Road, Leicester LE1 9HN, United Kingdom. E-mail: tph4@le.ac.uk.

C.E.M. and E.G. were supported by a Wellcome Trust Project Grant awarded to T.P.H. O.O. is supported by a Biotechnology and Biological Sciences Research Council/AstraZeneca Collaborative Awards in Science and Engineering studentship.

Disclosure Summary: The authors have nothing to disclose.

References

1. **Gomez E, Powell ML, Greenman IC, Herbert TP** 2004 Glucose-stimulated protein synthesis in pancreatic β-cells parallels an increase in the availability of the translational ternary complex (eIF2-GTP. Met-tRNAi) and the dephosphorylation of eIF2α. J Biol Chem 279:53937–53946
2. **Guest PC, Rhodes CJ, Hutton JC** 1989 Regulation of the biosynthesis of insulin-secretory-granule proteins. Co-ordinate translational control is exerted on some, but not all, granule matrix constituents. Biochem J 257:431–437
3. **Itoh N, Okamoto H** 1980 Translational control of proinsulin synthesis by glucose. Nature 283:100–102
4. **Itoh N, Sei T, Nose K, Okamoto H** 1978 Glucose stimulation of the proinsulin synthesis in isolated pancreatic islets without increasing amount of proinsulin mRNA. FEBS Lett 93:343–347
5. **Permutt MA** 1974 Effect of glucose on initiation and elongation rates in isolated rat pancreatic islets. J Biol Chem 249:2738–2742
6. **Permutt MA, Kipnis DM** 1972 Insulin biosynthesis: studies of islet polyribosomes (nascent peptides-sucrose gradient analysis-gel filtration). Proc Natl Acad Sci USA 69:505–509
7. **Harding HP, Zhang Y, Ron D** 1999 Protein translation and folding are coupled by an endoplasmic-reticulum-resident kinase. Nature 397:271–274
8. **Harding HP, Ron D** 2002 Endoplasmic reticulum stress and the development of diabetes: a review. Diabetes 51(Suppl 3):S455–S461
9. **Herbert TP** 2007 PERK in the life and death of the pancreatic β-cell. Biochem Soc Trans 35:1205–1207
10. **Harding HP, Novoa I, Zhang Y, Zeng H, Wek R, Schapira M, Ron D** 2000 Regulated translation initiation controls stress-induced gene expression in mammalian cells. Mol Cell 6:1099–1108
11. **Scheuner D, Song B, McEwen E, Liu C, Laybutt R, Gillespie P, Saunders T, Bonner-Weir S, Kaufman RJ** 2001 Translational control is required for the unfolded protein response and in vivo glucose homeostasis. Mol Cell 7:1165–1176
12. **Cullinan SB, Zhang D, Hannink M, Arvisais E, Kaufman RJ, Diehl JA** 2003 Nrf2 is a direct PERK substrate and effector of PERK-dependent cell survival. Mol Cell Biol 23:7198–7209
13. **Cullinan SB, Diehl JA** 2004 PERK-dependent activation of Nrf2 contributes to redox homeostasis and cell survival following endoplasmic reticulum stress. J Biol Chem 279:20108–20117
14. **Calfon M, Zeng H, Urano F, Till JH, Hubbard SR, Harding HP, Clark SG, Ron D** 2002 IRE1 couples endoplasmic reticulum load to secretory capacity by processing the XBP-1 mRNA. Nature 415:92–96
15. **Yoshida H, Matsui T, Yamamoto A, Okada T, Mori K** 2001 XBP1 mRNA is induced by ATF6 and spliced by IRE1 in response to ER stress to produce a highly active transcription factor. Cell 107:881–891
16. **Harding HP, Zhang Y, Bertolotti A, Zeng H, Ron D** 2000 Perk is essential for translational regulation and cell survival during the unfolded protein response. Mol Cell 5:897–904
17. **Senée V, Vattem KM, Delépine M, Rainbow LA, Haton C, Lecoq A, Shaw NJ, Robert JJ, Rooman R, Diatloff-Zito C, Michaud JL, Bin-Abbas B, Taha D, Zabel B, Franceschini P, Topaloglu AK, Lathrop GM, Barrett TG, Nicolino M, Wek RC, Julier C** 2004 Wolcott-Rallison Syndrome: clinical, genetic, and functional study of EIF2AK3 mutations and suggestion of genetic heterogeneity. Diabetes 53:1876–1883
18. **Back SH, Scheuner D, Han J, Song B, Ribick M, Wang J, Gildersleeve RD, Pennathur S, Kaufman RJ** 2009 Translation attenuation through eIF2α phosphorylation prevents oxidative stress and maintains the differentiated state in β cells. Cell Metab 10:13–26
19. **Gomez E, Powell ML, Bevington A, Herbert TP** 2008 A decrease in cellular energy status stimulates PERK-dependent eIF2α phosphorylation and regulates protein synthesis in pancreatic β-cells. Biochem J 410:485–493
20. **Michalak M, Robert Parker JM, Opas M** 2002 Ca^{2+} signaling and calcium binding chaperones of the endoplasmic reticulum. Cell Calcium 32:269–278
21. **Lodish HF, Kong N** 1990 Perturbation of cellular calcium blocks exit of secretory proteins from the rough endoplasmic reticulum. J Biol Chem 265:10893–10899
22. **Sambrook JF** 1990 The involvement of calcium in transport of secretory proteins from the endoplasmic reticulum. Cell 61:197–199
23. **Nakamura K, Bossy-Wetzel E, Burns K, Fadel MP, Lozyk M, Goping IS, Opas M, Bleackley RC, Green DR, Michalak M** 2000 Changes in endoplasmic reticulum luminal environment affect cell sensitivity to apoptosis. J Cell Biol 150:731–740
24. **Luciani DS, Gwiazda KS, Yang TL, Kalynyak TB, Bychkivska Y, Frey MH, Jeffrey KD, Sampaio AV, Underhill TM, Johnson JD** 2009 Roles of IP3R and RyR Ca^{2+} channels in endoplasmic reticulum stress and β-cell death. Diabetes 58:422–432
25. **Palmer AE, Jin C, Reed JC, Tsien RY** 2004 Bcl-2-mediated alterations in endoplasmic reticulum Ca^{2+} analyzed with an improved genetically encoded fluorescent sensor. Proc Natl Acad Sci USA 101:17404–17409
26. **MacLennan DH, Rice WJ, Green NM** 1997 The mechanism of Ca2+ transport by sarco(endo)plasmic reticulum Ca^{2+}-ATPases. J Biol Chem 272:28815–28818
27. **Hardie DG** 2003 The AMP-activated protein kinase cascade: the key sensor of cellular energy status. Endocrinology 144:5179–5183
28. **Novoa I, Zeng H, Harding HP, Ron D** 2001 Feedback inhibition of the unfolded protein response by GADD34-mediated dephosphorylation of eIF2α. J Cell Biol 153:1011–1022
29. **Harding HP, Zhang Y, Zeng H, Novoa I, Lu PD, Calfon M, Sadri N, Yun C, Popko B, Paules R, Stojdl DF, Bell JC, Hettmann T, Leiden JM, Ron D** 2003 An integrated stress response regulates amino acid metabolism and resistance to oxidative stress. Mol Cell 11:619–633
30. **Lu PD, Harding HP, Ron D** 2004 Translation reinitiation at alternative open reading frames regulates gene expression in an integrated stress response. J Cell Biol 167:27–33
31. **Vattem KM, Wek RC** 2004 Reinitiation involving upstream ORFs regulates ATF4 mRNA translation in mammalian cells. Proc Natl Acad Sci USA 101:11269–11274
32. **Lu PD, Jousse C, Marciniak SJ, Zhang Y, Novoa I, Scheuner D, Kaufman RJ, Ron D, Harding HP** 2004 Cytoprotection by preemptive conditional phosphorylation of translation initiation factor 2. EMBO J 23:169–179
33. **Jonas JC, Bensellam M, Duprez J, Elouil H, Guiot Y, Pascal SM** 2009 Glucose regulation of islet stress responses and β-cell failure in type 2 diabetes. Diabetes Obes Metab 11(Suppl 4):65–81
34. **Eizirik DL, Cardozo AK, Cnop M** 2008 The role for endoplasmic reticulum stress in diabetes mellitus. Endocr Rev 29:42–61
35. **Maechler P, Kennedy ED, Sebö E, Valeva A, Pozzan T, Wollheim CB** 1999 Secretagogues modulate the calcium concentration in the endoplasmic reticulum of insulin-secreting cells. Studies in aequorin-expressing intact and permeabilized ins-1 cells. J Biol Chem 274:12583–12592
36. **Tengholm A, Hellman B, Gylfe E** 1999 Glucose regulation of free Ca^{2+} in the endoplasmic reticulum of mouse pancreatic β cells. J Biol Chem 274:36883–36890
37. **Tengholm A, Hellman B, Gylfe E** 2001 The endoplasmic reticulum

is a glucose-modulated high-affinity sink for Ca^{2+} in mouse pancreatic β-cells. J Physiol 530:533–540
38. **Varadi A, Rutter GA** 2002 Dynamic imaging of endoplasmic reticulum Ca2+ concentration in insulin-secreting MIN6 Cells using recombinant targeted cameleons: roles of sarco(endo)plasmic reticulum Ca^{2+}-ATPase (SERCA)-2 and ryanodine receptors. Diabetes 51(Suppl 1):S190–S201
39. **Tarasov A, Dusonchet J, Ashcroft F** 2004 Metabolic regulation of the pancreatic β-cell ATP-sensitive K^+ channel: a pas de deux. Diabetes 53(Suppl 3):S113–S122
40. **Macdonald WA, Stephenson DG** 2006 Effect of ADP on slow-twitch muscle fibres of the rat: implications for muscle fatigue. J Physiol 573:187–198
41. **Macdonald WA, Stephenson DG** 2004 Effects of ADP on action potential-induced force responses in mechanically skinned rat fast-twitch fibres. J Physiol 559:433–447
42. **Macdonald WA, Stephenson DG** 2001 Effects of ADP on sarcoplasmic reticulum function in mechanically skinned skeletal muscle fibres of the rat. J Physiol 532:499–508
43. **Brostrom MA, Brostrom CO** 2003 Calcium dynamics and endoplasmic reticular function in the regulation of protein synthesis: implications for cell growth and adaptability. Cell Calcium 34:345–363
44. **Elouil H, Bensellam M, Guiot Y, Vander Mierde D, Pascal SM, Schuit FC, Jonas JC** 2007 Acute nutrient regulation of the unfolded protein response and integrated stress response in cultured rat pancreatic islets. Diabetologia 50:1442–1452
45. **Greenman IC, Gomez E, Moore CE, Herbert TP** 2007 Distinct glucose-dependent stress responses revealed by translational profiling in pancreatic β-cells. J Endocrinol 192:179–187
46. **Robertson R, Zhou H, Zhang T, Harmon JS** 2007 Chronic oxidative stress as a mechanism for glucose toxicity of the β cell in type 2 diabetes. Cell Biochem Biophys 48:139–146
47. **Asfari M, Janjic D, Meda P, Li G, Halban PA, Wollheim CB** 1992 Establishment of 2-mercaptoethanol-dependent differentiated insulin-secreting cell lines. Endocrinology 130:167–178
48. **Purkiss JR, Willars GB** 1996 Ionomycin induced changes in intracellular free calcium in SH-SY5Y human neuroblastoma cells: sources of calcium and effects on [3H]noradrenaline release. Cell Calcium 20:21–29